Main Physical Features and Processes Determining the Performance of Stationary Plasma Thrusters

Vladimir Kim*

Moscow Aviation Institute, Moscow 125810, Russia

The main physical features and processes determining stationary plasma thrusters (SPTs) performance levels are considered in this paper, including ionization processes and ion dynamics in the accelerating channel, as well as the results of SPT design optimization, factors determining SPT lifetime, and the possibilities of simulating the plasma particle dynamics in the accelerating channel and in its plume.

Nomenclature

B, B_r, B_{opt}	= magnetic field induction, its radial component, and the optimum B value, respectively
d, b_c	= accelerating channel mean diameter and its width, respectively
E, E_z	= electric field intensity and its z component, respectively
e	= electron charge
F	= thrust
h_c	= cycloid height, $2mE_z/eB_r^2$
I_d	= discharge current
I_i	= ion current
I_m	= current corresponding to the mass flow rate through the accelerating channel, $(\dot{m}_a/M)e$
j_{ez}	= z component of electron current density
j_H	= Hall current density
$j_\perp$	= normal ion current component at surface
$K_a, K_{a'}, K_h, K_w$	= numerical factor
K_M	= scaling factor
K_s	= sputtering yield factor
$K_\lambda \ll 1$	= numerical factor
K_ξ	= surface erosion rate factor
L_a	= length of accelerating channel
L_a^*	= length of the self-consistent accelerating layer
L_B	= characteristic width of $B_r(z)$ distribution
l, l_0	= magnetic system element sizes
M	= ion and atom mass
m	= electron mass
$\dot{m}, \dot{m}_a, \dot{m}_i$	= total mass flow rate in a thruster, mass flow rate through the accelerating channel, and mass flow rate of ions, respectively
N_a	= atom flow rate density, $n_a \cdot V_{az}$
N_d	= discharge power, $U_d \cdot I_d$
N_{sp}	= specific power, N_d/S_c
n_a, n_i, n_e	= concentrations of atoms, ions, and electrons, respectively
q	= ion charge
$\bar{r}, \Delta\bar{r}$	= normalized coordinates
$S_c \approx \pi d \cdot b_c$	= accelerating channel cross-sectional area
S_M	= magnetic core element cross-sectional area
$S_v(\gamma, \varepsilon_i)$	= volumetric sputtering yield
$\bar{S}_v(\gamma)$	= angular sputtering yield dependence factor, $S_v(\gamma, \varepsilon_i)/S_v(\gamma = 0, \varepsilon_i)$
t	= time
U^*	= minimal discharge voltage value with high efficiency of ionization
U_d	= discharge voltage
V, V_z	= heavy particle velocity in a plasma flow and its z component
V_{az}	= z component of mean value of the atom velocity
V_i, V_a	= ion and atom velocity, respectively
$\langle V_i \rangle, \langle V_i^2 \rangle$	= mean values of ion velocity and velocity squared, respectively
v_e	= electron velocity
x, y, z	= spatial coordinates
$\alpha, \langle\alpha\rangle$	= number of ionizations produced by an electron per unit length in z direction, and its mean value, respectively
β	= angle between ion velocity direction and the thruster axis
γ	= ion incident angle
$\varepsilon_i, \langle\varepsilon_i\rangle$	= energy of ions and their mean value
η_i	= thruster propellant usage efficiency, $\dot{m}_i/\dot{m}$
η_{ia}	= accelerator propellant usage efficiency, $\dot{m}_i/\dot{m}_a$
η_T	= thrust efficiency
η_{Ta}	= accelerator thrust efficiency
η_v	= efficiency, characterizing the spread of ions in velocities, $\langle V_i \rangle^2/\langle V_i^2 \rangle$
η_β	= focusing efficiency, $\langle V_z \rangle^2/\langle V_i \rangle^2$, $\langle\cos\beta\rangle^2$
η_ε	= efficiency of acceleration, $\langle\varepsilon_i\rangle/eU_d$, $M\langle V_i^2 \rangle/2eU_d$
ξ	= coordinate, normal to the discharge chamber wall surface
ν_e	= total electron collision frequency, $1/\tau$
$\nu_{ei}, \nu_{ea}, \nu_{ew}$	= frequency of electron collisions with ions, atoms, and walls, respectively
ν_i	= ionizational collision frequency
$\hat{O}_M$	= magnetic flow, $\int_{S_M} B \, dS_M$
ρ_{Le}	= electron Larmor radius
ρ_{Li}	= ion Larmor radius
$\sigma_i(v_e)$	= atom ionization cross section
$\langle\sigma_i v_e\rangle$	= ionization rate factor averaged through electron distribution function $f(v_e)$ in velocities, $\int_0^\infty \sigma_i(v_e)f(v_e)\, dv_e$
σ_0	= classical plasma conductivity, $ne^2\tau/m$, $ne^2/m\nu$
τ	= time between electron collisions
$\bar{\tau}$	= normalized time, τ/τ_0
$\varsigma, \Delta\varsigma$	= plasma potential and potential difference, respectively
ω	= electron cyclotron frequency, eB/m

$\omega\tau$ = Hall parameter
$(\omega\tau)_{\text{eff}}$ = effective $\omega\tau$ value

I. Introduction

ELECTRIC propulsion systems (EPSs) for spacecraft (S/C) maneuvering and orbit control are the new technology for improving S/C performance levels and increasing their capabilities because of the significantly higher specific impulses of EPSs in comparison with chemical propulsion systems. Extensive investigation and development were started at the end of the 1950s in the USSR, U.S., and other countries. As a result of these efforts, several types of electric thrusters were proposed, developed, and studied: electrostatic (ion) thrusters, plasma thrusters of different types, and electrothermal thrusters.[1] By the end of the 1960s, the performance of some of these thrusters had reached a relatively high level. However, because of the slower progress in space energetics and the great heritage of chemical propulsion, only a small number of electric thrusters with relatively low power became real competitors of the chemical systems. One of the first electric thrusters used in space technology after 1972 was the stationary plasma thruster (SPT), with a good performance level at specific impulses of 1000–3000 s. More than 100 SPTs have operated and still operate on Russian spacecraft, and the SPT-100-type thruster has been qualified according to the western standards.[2] It is expected that in the near future the propulsion subsystems based on this thruster will be widely used onboard western satellites. Many western experts are studying SPT physics and performance. Therefore, it seems useful to review the main SPT physical features leading to the high-performance level of this thruster. It is necessary to add that the physical processes in SPT (ionization, acceleration, ion beam formation, and neutralization) take place in conditions similar to those in the so-called thrusters with anode layer (TAL). Therefore, a consideration of these processes in the SPT could also be useful for studies of the TAL.

II. SPT Principle

The SPT functions on a relatively simple principle (Fig. 1); the gas flow goes through the annular accelerating channel formed by the discharge chamber walls and is ionized and accelerated in the electric discharge in the crossed electric and magnetic fields. The electric field is created by the voltage applied between an anode and a cathode-neutralizer. The quasiradial magnetic field is created by a magnetic system, generally consisting of magnetization coils, poles, and core.
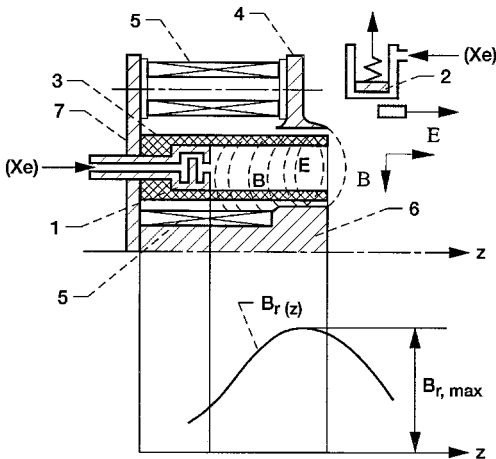

Fig. 1 Diagram of stationary plasma thruster: 1, anode-gas distributor; 2, cathode-neutralizer; 3, discharge chamber; 4, external pole; 5, coils of magnetization; 6, internal pole; 7, magnetic system-flange.

The magnetic induction value in the SPT accelerating channel is such that electrons are magnetized and ions are not magnetized, i.e.,

$$\rho_{Le} \ll L_a \ll \rho_{Li} \tag{1}$$

$$\omega\tau = \omega/\nu_e \gg 1 \tag{2}$$

Experimental data show that the ion energy is proportional to the difference $\Delta\varsigma$ in electric potential ς applied between the anode and cathode,[3] giving an ion velocity of

$$V_i \sim \sqrt{2q\Delta\varsigma/M} \tag{3}$$

Therefore, an acceleration of ions in the SPT accelerating channel is quasielectrostatic. The discharge plasma in the accelerating channel is quasineutral, however, so that ions are accelerated by the electric field created in the plasma volume. Therefore, there is no limitation on the ion current density by the space charge in the SPT accelerating channel, and ion flow and thrust density in the SPT are significantly higher than in the classical electrostatic thrusters. For example, in ion thrusters the typical ion current density is several mA/cm^2 at accelerating voltages of $\sim$ 1 kV, whereas in the SPT it is around 10^2 mA/cm^2 at accelerating (discharge) voltages $U_d \sim$ 100 V.

Accelerated ion flow exhausting the thruster channel catches the electrons emitted by the cathode and creates a reactive force

$$F = \dot{m}_i V_z \tag{4}$$

Assuming that the neutral atom velocity is negligible in comparison with the ion velocity and that all ions have a single charge, it is possible to obtain the following expression for the thrust efficiency:

$$\eta_T = \frac{\dot{m}_i V_z^2}{2N_d} = \frac{I_i}{I_d}\,\eta_i\eta_\beta\eta_v\eta_\varepsilon \tag{5}$$

Each multiplier on the right side of Eq. (5) characterizes a loss of energy in the thruster. For example, η_β characterizes the energy losses caused by plume divergence, and η_v reflects the loss caused by the wide spread of ions in velocities. If one considers the ionization losses, it is necessary to take into account not only the values of I_i/I_d and η_i; indirectly the ionization process also has an impact on the values of η_β, η_v, and η_ε. Similarly, an acceleration process has an impact on all of the multipliers on the right side of Eq. (5). This is natural because in a single-stage SPT the ionization and acceleration processes are closely connected. Therefore, to optimize the SPT performance it is necessary to optimize the entire complex of processes inside and outside the accelerating channel. Many efforts have been made to realize this optimization. Some results of these efforts are considered next.

III. Ionization and Ion Acceleration Processes

Ions appear in the accelerating channel because of gas atom ionization by electrons, coupling energy from the electric field. Their energy is typically higher than 10 eV, which is enough to ionize gas. Different types of cathodes can be used in a thruster, and so it is useful to consider the propellant usage efficiency in an accelerator separately, namely,

$$\eta_{ia} = \frac{\dot{m}_i}{\dot{m}_a} \approx \frac{I_i}{I_m} \approx \frac{I_i M}{\dot{m}_a e} \tag{6}$$

It is necessary to optimize the operation mode parameters to reach a high ionization efficiency. One of these parameters is the mass flow rate through the accelerating channel $\dot{m}_a$. Gas

ionization dynamics in a simplified form could be described by the following equation:

$$\frac{dn_a}{dt} = -\langle \sigma_i v_e \rangle n_e n_a \qquad (7)$$

Taking into account that neutral atom flow density, $N_a = n_a V_{az}$, $V_{az} dt = dz$, it is possible to write

$$\frac{dN_a}{N_a} = -\frac{\langle \sigma_i v_e \rangle n_e}{V_{az}} dz \qquad (8)$$

$$N_a(z) = N_{a0} \exp \left(-\int_0^z \frac{\langle \sigma_i v_e \rangle n_e}{V_{az}} d\xi \right) \qquad (9)$$

Assuming

$$\lambda_i(z) = \frac{V_{az}}{\langle \sigma_i v_e \rangle n_e} \approx \text{const} \qquad (10)$$

it is possible to obtain

$$N_a(z) = N_{a0} e^{-(z/\lambda_i)} = N_{a0} e^{-\alpha z} \qquad (11)$$

It is evident that to reach sufficient ionization efficiency, it is necessary to have

$$\lambda_i = K_\lambda \cdot L_a, \qquad (12)$$

where $K_\lambda \ll 1$.

For the operation modes with high ionization efficiency, it is possible to write

$$n_e \approx n_i \cong m_a/MV_i S_c \qquad (13)$$

Using Eqs. (12) and (13), one can obtain the restriction for the flow rate density through the accelerating channel

$$\frac{m_a}{M \cdot S_c} \geq \frac{V_i V_{az}}{\langle \sigma_i v_e \rangle K_\lambda L_a} \qquad (14)$$

So when operating under high enough flow densities and discharge voltages U_d, it is possible to obtain a high level of ionization efficiency. This conclusion is confirmed by experimental data (Fig. 2). The measured value of ion current I_i at the exit of the accelerating channel is very close to I_m with voltages $U_d \geq U^* = 120$ V, when the energy of the electrons is high enough and there is an adequate gas flow rate through the channel.

Considering Eq. (14), one can see that for alternative gases, such as Kr and Ar with comparable ion velocities (specific impulses), it is necessary to operate under higher specific flow rates, $m_a/M \cdot S_c$, because of the lowered σ_i and increased V_a
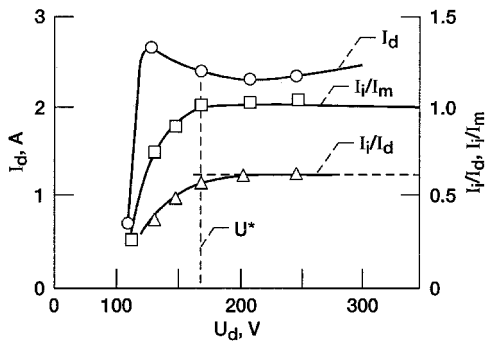

Fig. 2 Voltage–current characteristics of SPT.

values. This conclusion is also confirmed by the experimental data.

One of the parameters determining the efficiency of ionization is the electron energy controlled mainly by the discharge voltage. But the energy of the electrons depends not only on discharge voltage but also on the energy losses caused by atom ionization, excitation, and electron collisions with the walls, i.e., on the whole plasma dynamics inside the accelerating channel. At present, there is no model adequately describing the electron and plasma dynamics inside an accelerating channel because of the complexity of physical processes. Therefore, in practice, an experimental method is used to optimize thruster performance, taking into account the main thruster physical features.

In particular, to optimize an ionization process it is necessary to optimize the quantity of electrons going through the channel and coupling energy from the electric field. Ideally, this energy is equal to the value necessary for ionization of the full gas flow, and so it is necessary to control the electron current through the channel.

There are currently no fully proven models of electron transport across a magnetic field, despite several serious studies made in the 1960s and 1970s relating to the turbulent mechanisms of electron conductivity.[4-6] The problem is that these studies were made for the "old" SPT designs. The modern SPT has some different design features (see later in the text). As a result, the oscillation characteristics in the accelerating channel are also different from those studied earlier.

1) The intensity of the plasma oscillations in the frequency ranges 300 kHz–1 MHz is significantly lower than the intensity of oscillations in the frequency range 10 kHz–100 kHz. For the old design their relationship was the opposite.

2) The intensity of the low-frequency oscillations is maximal in the near-anode zone, but not in a zone with the maximal magnetic field induction.

The measurements of the Hall current density j_H and longitudinal electron current density j_{ez} allowed one to calculate the effective Hall parameter $(\omega\tau)_{\text{eff}} = j_H/j_{ez}$ value and to obtain $(\omega\tau)_{\text{eff}} \approx 200-300$ in a zone where Hall current is mainly located and where magnetic field induction is high enough.[8] This $\omega\tau$ value could be easily explained if one takes into account the scattering of electrons by the atoms and walls (the frequency of the electron collisions with atoms and walls is significantly higher than for electron–ion collisions in the channel).

Therefore, it is possible to use classical conductivity in a plasma at least in the part of the channel with high magnetic field induction values, where the accelerating layer is located. For the axisymmetrical channel configuration, where magnetic field induction B is directed along the radius (x axis), the electric field intensity is directed mainly along the z axis (parallel to the thruster axis, see Fig. 1) and the y axis is directed along the azimuthal direction of the channel, it is possible to obtain:

$$j_x = 0, \qquad E_x = -\frac{\nabla P_{ex}}{ne}, \qquad j_y = -\frac{\omega\tau\sigma_0 E_z^*}{1 + (\omega\tau)^2}, \qquad E_y = 0$$

$$\frac{\nabla P_{ey}}{ne} = 0, \qquad j_z = \frac{\sigma_0 E_z^*}{1 + (\omega\tau)^2}, \qquad E_z^* = E_z + \frac{\nabla P_{ez}}{ne} \qquad (15)$$

Taking into account that $\omega\tau \gg 1$, one can write

$$j_z \approx -(1/\omega\tau) j_y \qquad (16)$$

$$j_y \approx -ne(E_z^*/B) = -n v_{ey} e \qquad (17)$$

where

$$v_{ey} = E_z^*/B \qquad (18)$$

is the drift velocity, and

$$j_z \ll j_y \tag{19}$$

Therefore, electron movement could be interpreted as the so-called electric drift in "crossed" electric and magnetic fields. Under such consideration for the annular channel configuration the electron trajectories are almost closed. Therefore, the SPT and TAL are determined also as accelerators with closed electron drift.

The last equation in system (15) gives an expression for electron "heating" by an electric field in a hydrodynamic approximation. At the kinetic level, the collisions of the drifting electrons in the y direction cause their scattering by ions, atoms, and walls, and the transformation of their drift (directed) velocity component to the (nondirected) thermal one. Thus, collisions of electrons cause electron drift energy dissipation and the electric field repairs the drift velocity, adding additional energy to the electrons. This process gives the averaged shift of electrons in a z direction (to anode) at each collision with heavy particles and walls and explains both the electron transport across the magnetic field in the accelerating layer and the energy transfer from the electric field to the electrons.

From the preceding formulas it is clear that by controlling the magnetic field induction it is possible to control the electron current and to optimize its value. Practically, as a criterion for magnetic field optimization, the maximum magnitude $I_i/I_d = I_i/(I_i + I_e)$ can be considered (Fig. 3). If one takes into account that

$$\frac{I_i}{I_d} = \frac{I_i}{I_i + I_e} = \frac{1}{1 + (I_e/I_i)} \tag{20}$$

it is easy to understand that the requirement of $(I_i/I_d)_{max}$ is equivalent to the requirement of $(I_i/I_e)_{max}$, which means that such optimization gives the maximal ion yield per electron going from cathode to anode. Therefore, an increase in the magnetic field induction B to the B_{opt} value gives an increase in the ion yield (Fig. 3).

Concluding this consideration of the ionization process, it is necessary to add that according to the local plasma parameter measurements,[9] allowing an estimation of the ionization rate and energy losses for the ionization, the energy cost per ion in the SPT discharge is on the order of $3e\Phi_i$, where Φ_i is the gas atom ionization potential. And the total energy cost, taking into account the ion losses on the walls, is of the order of $(5-6)e\Phi_i$ per ion, i.e., $(60-70)$ eV/ion for the Xe case and $U_d \sim 200$ V. Thus, the SPT is a very effective ionizing device. This is one of the main reasons why the SPT has adequate thruster efficiency under moderate discharge voltages and I_{sp} values.

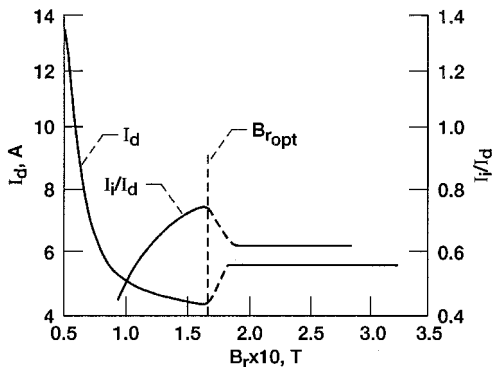To reach a high level of total efficiency, it is necessary not only to ionize and accelerate ions, but to accelerate them in the right direction. The main controlling factor in focusing ion flow is magnetic field topology.[10] The basis for this is that at low electron temperature levels the potential drop along the magnetic field lines is also small. Thus, the magnetic field lines of force are almost equipotential. Therefore, by changing the magnetic field topology it is possible to control the electric field structure and, correspondingly, the ion trajectories. But focusing the ion flow is a very complicated task because, according to relationship (15), there is a radial component of the electric field accelerating ions across the main direction of acceleration. Therefore, the real picture of the ion flow in the accelerating channel is very far from the ideal one (Fig. 4).[9] There are however, some possibilities for controlling the electric field equipotential line structure and ion trajectories in the accelerating channel by magnetic field topology optimization.

How the electric field intensity is distributed in the accelerating channel also is very important. According to Eq. (15), one can recognize that one of the external controlling factors is magnetic field induction, because the longitudinal component of electric conductivity is proportional to $1/(\omega\tau)^2$ and $\omega_e \sim B$. Therefore, the maximal values of E_z are to be realized in the part of the accelerating channel with maximal B values. Experimental data confirms this conclusion (Fig. 5).[9] Therefore, by changing the magnetic field induction distribution in the accelerating channel it is possible to control the electric field intensity distribution.

These two points determine the exclusive role of the magnetic field topology in the accelerating channel. From the beginning of SPT studies and development the idea was to focus the ion flow using the "focusing" type of magnetic field lines of force. As a result, the lens type of the magnetic field topology approximately symmetrical relative to the accelerating channel midsurface has been chosen (Fig. 6) as the basic one. For this type of magnetic field topology it is possible to use the mean value of the magnetic induction radial component gradient $\langle \nabla_z B_r \rangle$ along the mentioned surface as a measure of the magnetic field focusing properties, and experimental data[11] show (Fig. 7) that an increase in $\langle \nabla_z B_r \rangle$ reduces the SPT plume divergence characterized by the mean value of $\cos \beta$ ($\langle \cos \beta \rangle$
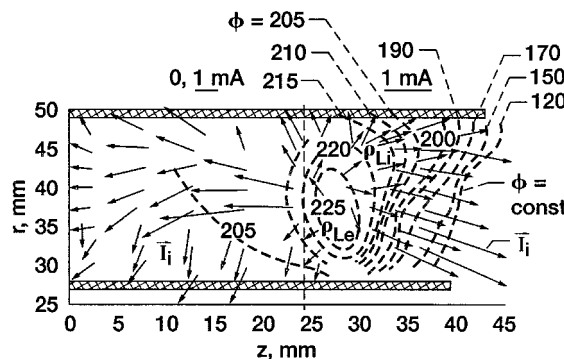

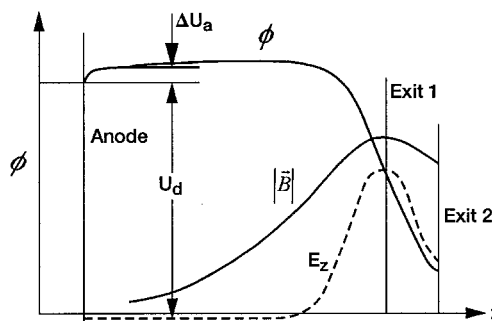Fig. 4 Diagram of ion currents I_i structure in an acceleration channel.

Fig. 5 Distribution of magnetic and electric fields along the channel.

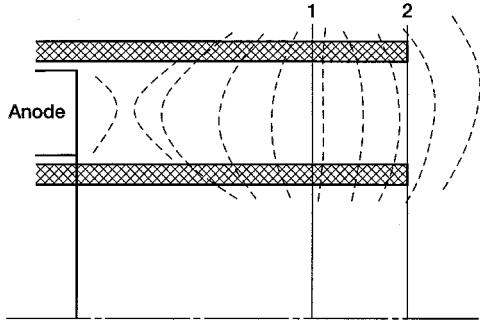Fig. 3 Discharge current and I_i/I_d ratio vs magnetic field induction.

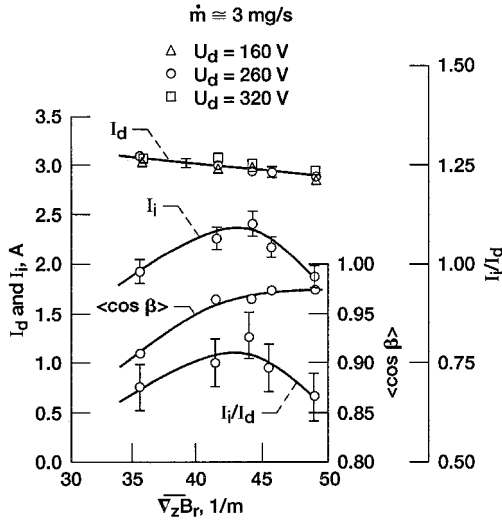Fig. 6 Magnetic field topology in the accelerating channel.

Fig. 7 Thruster papermeters vs $\langle \nabla_z B_r \rangle$: $\dot{m} = 3$ mg/s.

in Fig. 7) and ion losses on the walls indirectly characterized by the I_i/I_d value (see Fig. 7). Thus, by optimizing the magnetic field topology inside the SPT accelerating channel, it is possible to increase the thrust efficiency and to reduce its plume divergence because of an increase of at least I_i/I_d and η_β values [Eq. (5)]. In modern SPTs, such optimization has been realized.

IV. Optimized Modern SPT Features

As shown earlier, because of the significant radial electric field, part of the ions impinge on the discharge chamber walls. These ions lose their energy to the walls. Moreover, they are neutralized and leave the wall as neutral atoms. To achieve sufficient thruster efficiency, it is necessary to minimize these energy and particle losses. As explained earlier, a number of attempts were made to optimize the magnetic field topology and accelerating channel geometry to reduce losses. As a result, it was found that the optimal location of the magnetic lens is near the exit of the accelerating channel, where part of the accelerating layer is positioned inside the accelerating channel and part is outside it (see option I in Figs. 5 and 6).[11]

Moreover, it was found that for SPTs with optimized magnetic field topology there is a definite relationship between the magnetic layer characteristic size L_B, where magnetic induction is large enough, and the accelerating channel width b_c. It was also found that the accelerating layer longitudinal size L_a^*, where the electric field intensity is large enough, is in a first approximation proportional to L_B. Thus, it is possible to write

$$L_a^* \approx K_a \cdot L_B \tag{21}$$

$$L_{B\text{opt}} \approx K_B \cdot b_c \tag{22}$$

$$L_a^* \approx K_a' \cdot b_c \tag{23}$$

These relationships mean that under optimized operation modes of the optimized SPT the plasma interaction with the walls is at a definite level. So, it is possible to state that there is a similarity of processes in optimized SPTs of different sizes. This is understandable if one takes into account that in SPT plasma interaction with walls plays a significant role in the formation of the electron conductivity across the magnetic field and, correspondingly, in the formation of all other plasma parameter distributions in the accelerating channel.

It was shown also that it is possible to use the geometrical similarity of the main magnetic system elements and the discharge chamber,[11] permitting the simplification of the development of a new SPT model. The main geometrical parameter of the new SPT model in a first approximation can be chosen from a simple relationship using the corresponding parameter l_0 for the basic model:

$$l = K_M \cdot l_0 \tag{24}$$

In this case, the magnetic field topology for these models should be similar, and the optimized SPT performance is approximately the same for optimized models of different sizes. There are some particularities in the usage of similarity conditions. But, in general, these rules are very useful in SPT development, saving time and effort.

Typically, for the modern SPT, the accelerator thrust efficiency (calculated without cathode mass flow rate) is around 0.40 at a specific impulse $I_{sp} = 1200$ s, 0.55 at $I_{sp} \sim 1600$ s, 0.6 at $I_{sp} \sim 2000$ s, and 0.65–0.70 at $I_{sp} \sim 3000$ s. This conclusion cannot be extended to SPTs of reduced sizes because it is difficult to ensure the optimal magnetic field topology and magnetic field induction magnitude for such SPTs. This difficulty may be explained by the following.

As mentioned earlier, electron transport across the magnetic field in an accelerating layer could be interpreted as classical. Therefore, the electron current density j_{eo} at the exit of the accelerating channel or at the cathode side of the accelerating layer could be written as

$$j_{e0} = \frac{1}{(\omega_e \tau_e)_0} n_{e0} u_0 e = n_{e0} \frac{m E_{z0}}{e B_{r0}^2} v_{e0} e \tag{25}$$

where j_{e0}, n_{e0}, $(\omega_e \tau_e)_0$, u_0, ω_{e0}, v_{e0}, E_{z0}, and B_{r0} are the parameters at the referenced cross section. Assuming that in the accelerating layer the electric field intensity $E_z = $ const and the magnetic field induction $B_r = $ const, and that in other parts of the channel and in the plume $E_z = 0$ it is also possible to write in a layer

$$E_z \cong E_{z0} \cong U_d/L_a^* \tag{26}$$

where L_a^* is the longitudinal size of the self-consistent accelerating layer determined by the equilibrium between the ionization rate in the layer and the removal rate of the electrons by electron conductivity. According to Erofeev and Zharinov[12]

$$L_a^* \cong \sqrt{\frac{m U_d}{e B_r^2} \frac{v_e}{v_i}} \tag{27}$$

If the origin of the z coordinate is positioned at the exit of the thruster and the z axis is directed to the anode, an electron current density at the anode side of the accelerating layer is

$$j_{ea} = j_{e0} \exp\left[\int_0^{L_a^*} \alpha(z)\,dz\right] = j_{e0}\exp(\langle\alpha\rangle L_a^*) \tag{28}$$

The ion current density at the accelerating channel exit is

$$j_{i0} = j_{e0}[\exp(\langle\alpha\rangle L_a^*) - 1] \tag{29}$$

It is possible to suppose that

$$j_{ea} = j_d = I_d/S_c \tag{30}$$

Therefore, from relationships (27–29), one can obtain

$$\frac{j_{i0}}{j_d} = \frac{\exp(\langle\alpha\rangle L_a^*) - 1}{\exp(\langle\alpha\rangle L_a^*)} \tag{31}$$

It is possible to represent α as

$$\alpha \approx \frac{1}{\Delta}\frac{\nu_i}{\nu_e} = \frac{1}{k_h \cdot h_c}\frac{\nu_i}{\nu_e} \tag{32}$$

Taking into account relationships (25), (27), (29), and (30–32), one can obtain that in a first approximation

$$\langle\alpha\rangle L_a^* \approx 1/2\langle k_h\rangle \approx \text{const} \tag{33}$$

$$j_{i0}/j_{e0} \approx \text{const} \tag{34a}$$

$$j_{i0}/j_d \approx \text{const} \tag{34b}$$

Because under optimized operation modes with high enough voltages and mass flow rates

$$j_{i0} \approx j_m = me/MS_c \tag{35}$$

it is also possible to write that

$$j_d/j_m \approx \text{const} \tag{36}$$

That is, the SPT voltage–current characteristic general trend is very simple. This conclusion is confirmed in a first approximation by the experimental data (Fig. 2), although it is a very rough qualitative consideration. It is necessary to add that there is nothing specific to the SPT in this, and all of the preceding conclusions could also be extended to the TAL. Practice confirms this general point because all characteristics of the TAL and SPT are very similar.

Obviously, there are some differences in the SPT and TAL design and operations. The main difference in physics is a larger role of the plasma interaction with the walls in the case of the SPT.[1]

Returning to the SPT, one can take into account that

$$j_{i0} \approx n_{i0}V_{i0}e \approx n_{i0}\sqrt{(2eU_d/M)}e \tag{37}$$

Assuming that the energy of the electrons is proportional to the magnitude of U_d and the electron velocity $v_{e0} \sim \sqrt{U_d}$, that the magnitude of ν_{e0} is determined mainly by electron collisions with walls $[\nu_{e0} \sim (v_{e0}/b_c)]$, one can obtain from relationships (25), (34a) and (37)

$$U_d/B_r^2 L_a^* b_c \approx \text{const} \tag{38}$$

Or taking into account relationship (23), one can write

$$B_r \cdot b_c \approx \text{const} \quad \text{if} \quad U_d = \text{const} \tag{39a}$$

$$B_r \sim \sqrt{U_d} \quad \text{if} \quad b_c = \text{const} \tag{39b}$$

The necessity of increasing the magnetic field induction with the reduction of the characteristic channel (or thruster) size b_c causes an increase of the magnetic induction B_m in a magnetic core

$$B_m = \frac{\hat{O}_M}{S_M} \sim \frac{B_r b_c^2}{S_M} \sim \frac{(B_r b_c)b_c}{b_c^2} \sim \frac{1}{b_c} \tag{40}$$

Therefore, saturation of the magnetic core material does not allow the maintenance of the similarity condition [Eq. (24)] and the optimal magnetic field topology under reduced thruster size.

V. SPT Lifetime

There are at least several physical processes determining the SPT lifetime and reliability. Most of them, however, do not limit the possibility for the SPT lifetime to reach 7000 h or more.[10] The most intensive and visible process is the sputtering of the discharge chamber walls by accelerated ions. This process is sensitive to the thruster operation mode and corresponding power density. The rate of local discharge chamber wall surface deformation because of erosion can be determined by the expression

$$\dot{\xi} = j_\perp S_v(\gamma, \varepsilon_i) \tag{41}$$

As mentioned earlier, with respect to optimized SPT design and operation modes, the relative particle and energy losses on the walls are approximately constant, i.e., it is possible to write that

$$j_\perp \approx K_w j_m \tag{42}$$

In the range of discharge voltages that is most interesting for the near future, $U_d = (200–1000)$ V, the dependence of S_v on the ion energy ε_i is almost linear, and the ion energy ε_i is practically proportional to U_d.[13]

Therefore, it is possible to use the following approximation:

$$S_v(\gamma, \varepsilon) = S_V(\gamma, U_d) \approx K_s U_d \bar{S}_v(\gamma) \tag{43}$$

Expression (43) may be represented as the following:

$$\dot{\xi} = K_w(me/MS_c)\bar{S}v(\gamma)K_s U_d \sim (mU_d/S_c) \tag{44}$$

For the optimized SPT under optimal operation modes the discharge current $I_d \sim m$. Therefore,

$$\dot{\xi} \approx K_\xi \frac{I_d U_d}{S_c} \sim \frac{N_d}{S_c} \tag{45}$$

The last expression shows that the characteristic erosion rate in a first approximation is proportional to the power density in the accelerating channel.

Analysis of existing data on changes over time in the ion flow structure in the accelerating channel and in the discharge chamber wall profiles show that they are also in a first approximation similar for SPT models of different sizes.[14] If one uses the nondimensional linear sizes $\bar{z} = (z/l_e)$, $\Delta\bar{r} = (\Delta r/l_e)$, where z, $\Delta r(z)$, and l_e are the longitudinal coordinate of the surface point, the change of the surface radius corresponding to the z coordinate of surface, and the longitudinal size of the eroded part of surface, respectively, then the time dependence of $\Delta\bar{r} = f(\bar{\tau})$, where $\bar{\tau} = (\tau/\tau_0)$, i.e., normalized by the following factor:

$$\tau_0 = l_e/\dot{\xi}_0 = l_e/K_\xi I_d U_d \tag{46}$$

can be considered similar for optimized SPTs of different sizes. This time dependence can be represented by the formula

$$\Delta \bar{r} \approx c \bar{\tau}^{2/3} \qquad (47)$$

Numerical simulation of the erosion process under a typical ion flow structure and plasma parameters distribution in the accelerating channel shows that the dependence [Eq. (47)] is caused by this typical structure and by the mentioned distribution similarity.

Equation (47) is applicable up to a definite wear degree of the discharge chamber. Nevertheless, it seems possible to use it to obtain the expression for the estimated lifetime of SPTs of different sizes using data for the existing SPT,[14] namely

$$T = T_0 \left(\frac{N_{sp0}}{N_{sp}} \right) \left(\frac{\delta}{\delta_0} \right)^{3/2} \qquad (48)$$

where T_0, $N_{sp0} = N_0/S_{c0}$, and δ_0 are the lifetime, specific power, and wall thickness margin for the erosion for the existing thruster; and T, N_{sp}, and δ are the respective parameters for the new thruster.

Equation (48) was checked using lifetime data for the SPT-70 and SPT-100.[14] This is confirming the general similarity of erosion processes in modern SPTs.

VI. SPT Plume

In connection with the practical application of the SPT onboard S/C there are some integration issues to be solved. An operating SPT can interfere with S/C structural elements and subsystems in the following ways:

1) Mechanical impact of the operating SPT because of the appearance of SPT torque moments and interaction of its plume with the S/C elements.

2) Thermal interference of the SPT structure with the S/C body and thermal impact of the energy release on the surfaces of structural S/C elements if they intersect with the SPT plume.

3) Sputtering of structural S/C elements if they intersect with the SPT plume.

4) Contamination because of the deposition of sputtered and evaporated materials from the SPT structural elements.

5) Change of the S/C's "own" atmosphere due to release of gas and plasma flow from the operating SPT and EPS.

6) Electrostatic environment change because of SPT operation.

7) Electromagnetic interference of the operating SPT and its plume with the other S/C subsystems.

Analysis of these impacts and experience with SPT usage on board Russian S/C shows that all these impacts can be reduced to an acceptable level by careful positioning of thrusters and orientation of their axes. However, to solve this problem accurately it is necessary to know the SPT plume parameters distribution at least. Therefore, a significant part of the R&D effort has been spent on the theoretical and experimental

Fig. 8   Streamlines of ions (simulation).

study of the plume. As a result of these studies, there is now more or less full information on the accelerated ion current density and their mean energy spatial distributions in the plume.[15] But experimental measurements do not give full data on the plume parameters. Therefore, a theoretical plume model is now being developed in Russia and in the U.S. Model development at the RIAME MAI[16] is based on the plasma flow dynamics description, with the kinetic equations for ions and atoms as well as for the surrounding gas atoms. This last could be immobile or directed into to the thruster exit plane. Using the model it is also possible to simulate the dynamics of the recharged particles in a plume and particles sputtered from the discharge chamber walls.

In particular the appearance of the ion backflow (Fig. 8) due to the recharging of ions was shown.[16] The kinetic equation approach for the description of all the plasma particle dynamics, including electrons, is under development at RIAME MAI. The authors of this approach hope that it will give the full picture of the ionization and acceleration processes in the accelerating channel.

VII. Conclusions

The data presented here show that theoretical and experimental investigations of the physical processes in the SPT have provided a significant amount of information on factors determining SPT performance. There are still, however, many questions about the physics of SPT operation, including the full description of the plasma dynamics and the physics of the plasma instabilities and their impact on the other processes. Therefore, further investigations are planned.

References

[1]Bober, A. S., Kim, V., Koroteev, A. S., Latyshev, L. A., Morozov, A. I., Popov, G. A., Rylov, Yu. P., and Zhurin, V. V. "State of the Works on Electrical Thrusters in USSR," *Proceedings of the 22nd International Electric Propulsion Conference* (Viareggio, Italy), 1991 (IEPC Paper 91-003).

[2]Arkhipov, B. A., Vinogradov, V. N., Kozubsky, K. N., Kudryavtsev, S. S., Maslennikov, N. A., and Murashko, V. M., "Development and Application of Electric Thrusters at EDB Fakel," International Electric Propulsion Conf., IEPC Paper 97-04, Cleveland, OH, Aug. 1997.

[3]Morozov, A. I., Esipchuk, Yu. V., Tilinin G. N., Trofimov, A. V., Sharov, Yu. A., and Shepkin, G. Ya., "Experimental Investigation of the Plasma Accelerator with Closed Drift of Electrons and Extended Acceleration Zone," *Journal of Technical Physics*, Vol. XLII, No. 1, 1972, pp. 54–63 (in Russian).

[4]Morozov, A. I., Esipchuk Yu. V., Kapulkin, A. M., Nevrovsky, V. A., and Smirnov, G. G., "Azimuthally Nonsymmetric Oscillations and Anomalous Conductivity in the Accelerators with Closed Drift of Electrons," *Journal of Technical Physics*, Vol. XLII, No. 5, pp. 972–982, 1973 (in Russian).

[5]Esipchuk, Y. V., and Tilinin, G. N., "The Drift Plasma Instability in ACDE," *Journal of Technical Physics*, Vol. XLVI, No. 4, 1976, pp. 718–729 (in Russian).

[6]Tilinin G. N., "Experimental Investigation of the High Frequency Oscillations in A CDE," *Journal of Technical Physics*, Vol. XLVII, No. 8, 1977, pp. 1684–1691 (in Russian).

[7]Bishaev, A. M., Gavryushin, V. M., Gerasimov, V. F., Kim, V., Kozlov, V. I., Shishkin, G. G., "Investigation of the Oscillations in a Discharge Circuit and the Channel Wall Conductivity on Processes in a ACDE," *Book of Abstracts of the IVth All Union Conference on Plasma Accelerators and Ion Injectors*, All Union Scientific and Technological Information Center, Moscow, Russia, 1978, pp. 57–58, (in Russian).

[8]Bishaev, A. M., and Kim, V., "Investigation of the Local Plasma Parameters in an Accelerator with Closed Drift of Electrons and Extended Acceleration Zone," *Journal of Technical Physics*, Vol. XLVIII, No. 9, 1978, pp. 1853–1857 (in Russian).

[9]Bugrova, A. I., and Kim, V., "The Modern Status of Physical Investigations in Accelerators with Closed Electron Drift and Extended Acceleration Zone," *Plasma Accelerators and Ion Injectors*, edited by L. A. Artsimovich, Nauka, Moscow, 1984, pp. 107–129 (in Russian).

[10]Morozov, A. I., "Electric Propulsion Thrusters and Plasmadynamics," *Proceedings of the 24th International Electric Propulsion*
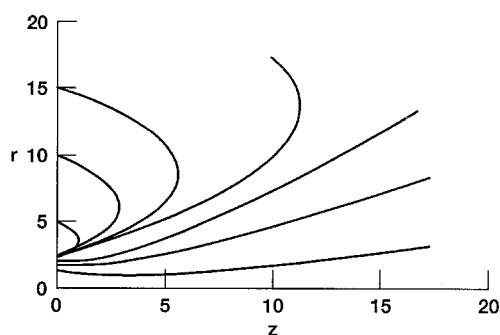
Conference (Moscow), 1995, pp. 41–53 (IEPC Paper 95-05).

[11]Gavryushin, V. M., Kim, V., Kozlov, V. I., and Maslennikov, N. A., ''Physical and Technical Bases of the Modern SPT Development,'' *Proceedings of the 24th International Electric Propulsion Conference*, Moscow State Aviation Institute, Moscow, Russia, 1995, pp. 307–314 (IEPC Paper 95-38).

[12]Erofeev, V. S., and Zharinov, A. V. ''Ion Acceleration in the EH Sheath with Closed Hall Current,'' *Plasma accelerators*, Mashinostroenie, Moscow, 1972, pp. 65–67 (in Russian).

[13]Abgaryan, V., Kaufman, H., Kim, V., Ovsyanko, D., Shkarban, I., Semenov, A., Sorokin, A., Zhurin, V., ''Calculation Analysis of the Erosion of the Discharge Chamber Walls and Their Contamination During Prolonged SPT Operation,'' AIAA Paper 94-2859, June 1994.

[14]Clauss, C., Day, M., Kim, V., Kondakov, Yo., and Randolph, Th., ''Preliminary Study of Possibility to Ensure Large Enough Life Time of SPT Operating Under Increased Powers,'' AIAA Paper 97-2789, July 1997.

[15]Absalamov, S. K., Andreev, V. B., Colbert, T., et al., ''Measurement of Plasma Parameters in the Stationary Plasma Thruster (SPT-100) Plume and Its Effect on Spacecraft Components,'' AIAA Paper 92-3156, July 1992.

[16]Bishaev, A. M., Kalashnikov, V. K., Kim, V., and Shavykina, A. V., ''The Simulation of the Sputtered Particle Dynamics in the SPT Plume,'' *Proceedings of the 2nd European Spacecraft Propulsion Conference*, European Space Agency, Nordwijk, The Netherlands, 1997, pp. 349–354.